Solution of voter model dynamics on annealed small-world networks

Daniele Vilone*

*Dipartimento di Fisica, Università di Roma "La Sapienza," and SMC-INFM, Unità di Roma 1,
Piazzale Aldo Moro 2, I-00185 Roma, Italy*

Claudio Castellano†

Dipartimento di Fisica, Università di Roma "La Sapienza," and INFM, Unità di Roma 1, Piazzale Aldo Moro 2, I-00185 Roma, Italy

An analytical study of the behavior of the voter model on the small-world topology is performed. In order to solve the equations for the dynamics, we consider an annealed version of the Watts-Strogatz (WS) network, where long-range connections are randomly chosen at each time step. The resulting dynamics is as rich as on the original WS network. A temporal scale τ separates a quasistationary disordered state with coexisting domains from a fully ordered frozen configuration. τ is proportional to the number of nodes in the network, so that the system remains asymptotically disordered in the thermodynamic limit.

I. INTRODUCTION

The relationship between nontrivial interaction topologies and ordering phenomena is still a largely unexplored topic. The recent burst of activity on complex networks has revealed that many technological, social, and biological systems have interaction patterns markedly different from structures traditionally studied as regular lattices and random graphs [1,2]. The interest is now focusing on how such complex topologies affect dynamical processes taking place on them. Models of ordering dynamics play an important role in this context, since they are commonly used to study social phenomena, such as cultural assimilation and opinion dynamics [3–6], for which the interaction patterns are more plausibly described by complex networks than by regular lattices.

Some ordering processes on complex networks have recently been considered, including the zero-temperature Glauber dynamics of the Ising model on the Watts-Strogatz network [7] and the Axelrod model on small-world and scale-free networks [8].

In a recent paper [9], we have studied numerically the dynamics of the voter model on a small-world network. This structure, more precisely the Watts-Strogatz (WS) network [10], is one of the simplest examples of complex topology. Depending on the parameter p (to be specified below) it interpolates between a one-dimensional lattice with periodic boundary conditions (for $p=0$) and a random graph (for $p=1$). It has been shown [10] that in a well-defined range of intermediate values of p, the network has, simultaneously, global properties typical of random graphs (small average distance between nodes) and local properties (clustering) typical of regular structures.

The voter model is possibly the simplest model of an ordering process [11]. On each site a discrete variable σ is

defined, which may assume two values ($\sigma=\pm1$) representing two opposite options, for instance, the electoral choice in favor of two different candidates. Starting from a disordered initial condition, the model follows a simple dynamical evolution: at each time step one site is selected at random and set equal to one of its nearest neighbors, chosen at random in its turn. On regular lattices, in $d=1$ and $d=2$, the model converges to an ordered state with all variables having the same value, whereas for $d \geqslant 3$ the system reaches a disordered stationary state [12,13]. The voter model on complete graphs has been considered recently [14,15].

In Ref. [9] we have found that the nontrivial connectivity pattern of the WS network has a deep impact on the ordering dynamics of the voter model. In particular, after an initial transient, the system settles in a quasistationary state with coexisting domains. If the system size is infinite, this state persists forever: at odds with naive expectations, long-range connections prevent complete ordering from being reached. If the system size is kept finite instead, the stationary state has a finite lifetime and the fully ordered state is quickly reached at the end of it. Interestingly, the dependence of the lifetime on the system size is such that the ordered state is reached earlier than on a one-dimensional lattice of the same size. This partially restores the intuitive picture that long-range connections should speed up the ordering process.

In this work we analyze the same problem from the analytical point of view. The very simple form of the transition rates for the voter model results in equations of motion for the correlation functions that are not coupled with each other. The only difficulty is to carry out the average over trajectories for a fixed realization of the network and to average over the topology afterward. To overcome this problem we use an annealed approximation, consisting in averaging over the topology before averaging over the trajectories. This approximation is exact for an effective network, which we call annealed WS network, where long-range interactions are not quenched from the beginning but are extracted randomly at each time step. The dynamics of the voter model on the annealed WS network is then solved, revealing a phenom-

_____

*Electronic address: daniele@pil.phys.uniroma1.it

†Electronic address: castella@pil.phys.uniroma1.it

enology as rich as in the quenched case. By comparing the exact results on the annealed WS network with the numerical simulations on the quenched one, it turns out that the only discrepancy between the two cases is the dependence on the parameter p of the correlation length in the stationary disordered state.

The paper is organized as follows. In the following section we define precisely the voter model dynamics and the WS topology on which the process occurs. Section III is devoted to the analytical solution of the dynamics. The equation of motion for the correlation function is derived, the annealed approximation is introduced, and the behavior of the system is studied. In Sec. IV we check numerically the analytical results for the annealed case and compare them with simulations of the quenched case. In Sec. V we extend the results to the case where each site is initially connected to 2ν neighbors. The final section contains a short discussion of the findings.

II. THE MODEL

We consider a small-world network defined as the superposition of a one-dimensional lattice of L sites with periodic boundary conditions and a random graph [16]. In general, one can start from a lattice with each site linked to ν neighbors on the right and ν on the left. We now consider $\nu=1$, deferring the discussion of generic values of ν to Sec. V. More precisely, site i is initially connected with sites $i-1$ and $i+1$. Then a link is added between any pair of non-nearest neighbor sites with probability p/L. In this way the total number of edges in the system is $L+[L(L-3)/2]p/L$, so that the average degree per site is finite ($2+p$) in the thermodynamic limit $L\rightarrow\infty$. The generalization to an initial lattice with connections to k nearest neighbors is straightforward. This topology slightly differs from the one originally introduced by Watts and Strogatz [10] but has the same properties and is more amenable to analytical treatment. The topology is fully specified by the adjacency matrix $Q(i,j)$, which is 1 if i and j are connected and 0 otherwise. The probability distribution of its elements is

$$P[Q(i,j)]=\begin{cases} \delta_{Q(i,j),0} & \text{for } i=j \\ \delta_{Q(i,j),1} & \text{for } i=j\pm1 \\ \dfrac{p}{L}\delta_{Q(i,j),1}+\left(1-\dfrac{p}{L}\right)\delta_{Q(i,j),0} & \text{otherwise.} \end{cases}$$

(1)

The voter model dynamics is defined by the transition rates. If we call $\{\sigma\}$ the spin configuration of the system, that is, $\{\sigma\}=\{\sigma_1,\sigma_2,\ldots,\sigma_i,\ldots,\sigma_L\}$ and we indicate with $\{\sigma'\}_i$ the same configuration with the ith spin flipped, the transition rate from state $\{\sigma\}$ to state $\{\sigma'\}_i$ is, in complete analogy with the definition for regular lattices,

$$w(\{\sigma\}\rightarrow\{\sigma'\}_i)=\frac{1}{2}\left(1-\frac{\sigma_i}{z_i}\sum_k Q(i,k)\sigma_k\right),$$

(2)

where z_i, the degree of site i, is

$$z_j=\sum_i Q(i,j).$$

III. ANALYTICAL TREATMENT

A. Equation for the correlation function

Given the explicit expression (2) of the transition rates, from the master equation

$$\frac{d}{dt}P(\{\sigma\},t)=\sum_i w(\{\sigma'\}_i\rightarrow\{\sigma\})P(\{\sigma'\}_i,t)-\sum_i w(\{\sigma\}$$
$$\rightarrow\{\sigma'\}_i)P(\{\sigma\},t),$$

(3)

one can derive [17,18] the equation of motion for the mean spin at site j, $s_j\equiv\langle\sigma_j\rangle$,

$$\frac{ds_j}{dt}=-s_j+\sum_k \frac{Q(j,k)s_k}{z_j},$$

(4)

and for the two-point correlation function $C_{j,k}\equiv\langle\sigma_j\sigma_k\rangle$,

$$\frac{dC_{j,k}}{dt}=-2C_{j,k}+\sum_i \frac{Q(j,i)C_{k,i}}{z_j}+\sum_i \frac{Q(k,i)C_{j,i}}{z_k}.$$

(5)

For $p=0$, Eqs. (4) and (5) coincide with the equations for the one-dimensional voter model [13].

In order to study the dynamics of the voter model on the Watts-Strogatz network, we must average Eqs. (4) and (5) over the disordered topology. Indicating with an overbar the averaged quantities $\bar{A}=\int\Pi_{i,j}dQ(i,j)AP[Q(i,j)]$, the equation for the mean spin is

$$\frac{d\bar{s}_j}{dt}=-\bar{s}_j+\sum_k \overline{\left(\frac{Q(j,k)s_k}{z_j}\right)},$$

(6)

and the one for the pair correlation function is

$$\frac{d\bar{C}_{j,k}}{dt}=-2\bar{C}_{j,k}+\sum_i \overline{\left(\frac{Q(j,i)C_{k,i}}{z_j}\right)}+\sum_i \overline{\left(\frac{Q(k,i)C_{j,i}}{z_k}\right)}.$$

(7)

To evaluate the average values appearing on the right-hand side of Eqs. (6) and (7) we introduce the annealed approximation

$$\overline{\left(\frac{Q(j,k)}{z_j}\right)A}=\overline{\left(\frac{Q(j,k)}{z_j}\right)}\bar{A}.$$

(8)

This approximation can be seen as considering annealed transition rates

$$\bar{w}(\{\sigma\}\rightarrow\{\sigma'\}_i)=\frac{1}{2}\left[1-\sum_k \overline{\left(\frac{Q(i,k)}{z_i}\right)}\sigma_i\sigma_k\right].$$

(9)

The evaluation of $\overline{(Q(j,k)/z_j)}$ is readily performed:

$$\overline{\left(\frac{Q(j,k)}{z_j}\right)} = \int \prod_{l,m} dQ(l,m) P[Q(l,m)] \frac{Q(j,k)}{\sum_i Q(j,i)}$$

$$= \int dQ(j,k) P[Q(j,k)] Q(j,k)$$

$$\times \int \prod_{l,m \neq j,k} dQ(l,m) P[Q(l,m)] \frac{1}{\sum_i Q(j,i)}. \tag{10}$$

Inserting Eq. (1) in Eq. (10), one easily finds for $k=j$,

$$\overline{\left(\frac{Q(j,j)}{z_j}\right)} = 0, \tag{11}$$

for $k = j \pm 1$,

$$\overline{\left(\frac{Q(j,j \pm 1)}{z_j}\right)} = \int dQ(j,k) P[Q(j,k)] Q(j,k)$$

$$\times \sum_{n=0}^{L-3} \binom{L-3}{n} \frac{(p/L)^n (1-p/L)^{L-3-n}}{1+Q(j,k)+n}$$

$$= f_2(p/L, L-3), \tag{12}$$

and, similarly, for $k \neq j, j \pm 1$,

$$\overline{\left(\frac{Q(j,k)}{z_j}\right)} = \frac{p}{L} f_3(p/L, L-4), \tag{13}$$

where

$$f_R(\alpha, N) = \sum_{n=0}^{N} \binom{N}{n} \frac{\alpha^n (1-\alpha)^{N-n}}{R+n}. \tag{14}$$

Explicit formulas for the functions f_2 and f_3 are given in the Appendix. In the limit of large L they tend to the simple forms

$$F_2(p) = \lim_{L \to \infty} f_2(p/L, L-3) = \frac{1}{p} - \frac{(1-e^{-p})}{p^2}$$

and

$$F_3(p) = \lim_{L \to \infty} f_3(p/L, L-4) = \frac{1}{p} - \frac{2}{p^2} + \frac{2(1-e^{-p})}{p^3},$$

which go to 1/2 and 1/3, respectively, in the limit $p \to 0$.

The dynamical rule corresponding exactly to rates (9) is easily found. At each time step one site (site i) of a one-dimensional lattice is randomly selected. Then, with probability $f_2(p/L, L-3)$ one of the two nearest neighbors ($i+1$ or $i-1$) is chosen and σ_i is set equal to it. With probability $(p/L)f_3(p/L, L-4)$ instead, one randomly chooses one of the other $L-3$ sites and sets σ_i equal to it. In this way, the effective topology over which the dynamics takes place changes at each time step. We call such network "annealed" WS network. The average properties are those of the original "quenched" WS network, but no permanent connection exists between non nearest neighbor sites.

We can now write down the explicit form of the equations of motion for the mean spin and the correlation function on the annealed Watts-Strogatz network as

$$\dot{s}_j = -s_j + f_2(p/L, L-3)(s_{j+1} + s_{j-1})$$

$$+ \frac{p}{L} f_3(p/L, L-4) \sum_{l \neq j, j \pm 1} s_l, \tag{15}$$

$$\dot{C}_{j,k} = -2C_{j,k} + f_2(p/L, L-3)(C_{j+1,k} + C_{j-1,k} + C_{j,k+1}$$

$$+ C_{j,k-1}) + \frac{p}{L} f_3(p/L, L-4)$$

$$\times \left(\sum_{l \neq j, j \pm 1} C_{k,l} + \sum_{l \neq k, k \pm 1} C_{j,l} \right). \tag{16}$$

For simplicity, here and in the following, the overbar is omitted. Also the arguments of f_2 and f_3 will often be omitted.

Equation (16) is complemented by the boundary condition $C_{j,j} = 1$ and by the initial condition $C_{j,k}(t=0)$. We consider an initial fully uncorrelated state $C_{j,k}(t=0) = \delta_{j,k}$. Hence the correlation function depends only on $r = |j-k|$ for all times, and the equation of motion is

$$\dot{C}(r) = -2 \left(1 + \frac{pf_3}{L} \right) C(r) + 2 \left(f_2 - \frac{pf_3}{L} \right)$$

$$\times [C(r+1) + C(r-1)] + 2 \frac{pf_3}{L} \sum_{l=0}^{L-1} C(l), \tag{17}$$

where the relation $2f_2(p/L, L-3) + (L-3)p/Lf_3(p/L, L-4) - 1 = 0$, proved in the Appendix [Eq. (A4)], has been used.

If we sum Eq. (15) over j and divide by L, we obtain the temporal evolution of average total magnetization $M = (1/L)\sum_j s_j$:

$$\frac{dM}{dt} = [-1 + 2f_2(p/L, L-3)$$

$$+ (L-3)p/Lf_3(p/L, L-4)]M. \tag{18}$$

Since the coefficient on the right-hand side vanishes [Eq. (A4)] the average total magnetization is conserved, as in the dynamics on regular lattices.

B. The stationary state

We now turn to the analysis of Eq. (17) and consider first the continuum limit in real space, yielding

$$\dot{C} = -2(1-2f_2)\left(1+\frac{3}{L-3}\right)C + 2\left(f_2 - \frac{1-2f_2}{L-3}\right)C''$$

$$+2\frac{1-2f_2}{L-3}\int_0^L dr C(r). \tag{19}$$

Let us look for final configurations of the system, i.e., solutions of the stationary equation

$$C'' - \lambda_L^2 C + \Phi_L = 0, \tag{20}$$

where

$$\lambda_L^2 = \frac{(1-2f_2)[1+3/(L-3)]}{[f_2 - (1-2f_2)/(L-3)]} > 0 \tag{21}$$

and

$$\Phi_L = \frac{\lambda_L^2}{L}\int_0^L dl C(l). \tag{22}$$

For finite L, taking into account that $C(r=0)=1$ and $|C(r)| \leq 1 \forall r$, one obtains

$$C(r) = \frac{\Phi_L}{\lambda_L^2} + \left[1 - \frac{\Phi_L}{\lambda_L^2}\right]\exp(-\lambda_L r). \tag{23}$$

Imposing the consistency of Eq. (23) with Eq. (22), the final correlation function turns out to be

$$C(r) = 1 \quad \forall r \geq 0. \tag{24}$$

The final configuration of the system is a frozen fully ordered state.

On the other hand, in the thermodynamic limit $L \rightarrow \infty$, $(1/L)\int_0^L dr C(r) = C(\infty)$ so that the solution is

$$C(r) = C(\infty) + [1 - C(\infty)]\exp[-\lambda(p)r], \tag{25}$$

with $\lambda^2(p) = \lim_{L\rightarrow\infty}\lambda_L^2$. From Eq. (19) one obtains $\dot{C}(\infty) = 0$, and since $C(\infty) = 0$ for $t=0$ we have

$$C(r) = \exp[-\lambda(p)r]. \tag{26}$$

Hence the stationary configuration of the system is disordered, with a correlation length ξ_p,

$$\xi_p = \frac{1}{\lambda(p)} = \frac{1}{\sqrt{1/F_2(p)-2}} = \frac{1}{\sqrt{p^2/(p-1+e^{-p})-2}}, \tag{27}$$

where the explicit form of $F_2(p) = \lim_{L\rightarrow\infty}f_2(p/L, L-3)$ is computed in the Appendix. In the limit of small p the correlation length diverges as $p^{-1/2}$.

C. Preasymptotic dynamics

We now study the equation of motion (17) in Fourier space by closely following the treatment for the Ising model

on a one-dimensional lattice [19]. In this way, not only the stationary state but also the preasymptotic dynamics can be analyzed. Introducing

$$C(r,t) = \frac{1}{L}\sum_{k'} c_{k'}(t)e^{ik'r}, \tag{28}$$

with $k' = 2\pi n/L$, $n = -L/2, \ldots, L/2$, multiplying both sides of Eq. (17) by e^{-ikr}, and summing over r from 1 to $L-1$, we obtain

$$\frac{1}{L}\sum_{k'}\dot{c}_{k'}(t)\sum_{r=1}^{L-1}e^{i(k'-k)r}$$

$$= -2A\frac{1}{L}\sum_{k'}c_{k'}(t)\sum_{r=1}^{L-1}e^{i(k'-k)r} + 2B\frac{1}{L}\sum_{k'}c_{k'}(t)$$

$$\times(e^{ik'}+e^{-ik'})\sum_{r=1}^{L-1}e^{i(k'-k)r} + 2\frac{p}{L}f_3 C_0\sum_{r=1}^{L-1}e^{-ikr}.$$

Using $\sum_{r=1}^{L-1}e^{i(k-k')} = L\delta_{k,k'} - 1$, we get

$$\dot{c}_k(t) = -\gamma_k c_k(t) + A(t) + 2\frac{pf_3}{L}c_0(t)(L\delta_{k,0}-1), \tag{29}$$

where

$$\gamma_k = 2\left[1 + \frac{pf_3}{L} - 2\left(f_2 - \frac{pf_3}{L}\right)\cos(k)\right] \tag{30}$$

and

$$A(t) = \frac{1}{L}\sum_k c_k(t)\gamma_k. \tag{31}$$

The disordered initial condition implies $c_k(t=0)=1$ for all k. The boundary condition $C(r=0,t)=1$ implies

$$1 = \frac{1}{L}\sum_k c_k(t) \tag{32}$$

for all t. Equation (29) can be solved by Laplace transform methods. Introducing

$$\hat{c}_k(s) = \int_0^\infty c_k(t)e^{-st}dt. \tag{33}$$

Equation (29) becomes

$$s\hat{c}_k(s) - 1 = -\gamma_k\hat{c}_k(s) + \hat{a}(s) + 2pf_3\hat{c}_0(s)(\delta_{k,0}-1/L), \tag{34}$$

where $\hat{a}(s) = L^{-1}\sum_k\gamma_k\hat{c}_k(s)$ is the Laplace transform of $A(t)$. The coefficients $\hat{c}_k(s)$ can be formally written down as

$$\hat{c}_k(s) = \begin{cases} \dfrac{\hat{a}(s)+1}{s+\gamma_0/L}, & k=0 \\[3mm] \dfrac{\hat{a}(s)+1-\gamma_0\hat{c}_0(s)/L}{s+\gamma_k}, & k\neq 0. \end{cases} \tag{35}$$

Note that $\gamma_0 = 2pf_3$. To determine $\hat{a}(s)$ we transform the boundary condition (32), use the expressions (35), and replace the discrete sum over k with an integral (which is correct in the limit of large L we are interested in), obtaining

$$\frac{1}{s} = \frac{\hat{a}(s)+1}{Ls+\gamma_0} + \left(1 - \frac{\gamma_0}{Ls+\gamma_0}\right)[\hat{a}(s)+1]\int_{-\pi}^{\pi}\frac{dk}{2\pi}\frac{1}{s+\gamma_k}. \quad (36)$$

For large L we can take $\gamma_k(L) \rightarrow \gamma_k(L=\infty) = 2[1-(1-\gamma_0/2)\cos(k)]$. The integral is easily carried out yielding $(s^2+4s+4[1-(1-\gamma_0/2)^2])^{-1/2}$. We are interested in $t \gg 1/p \Rightarrow s \ll \gamma_0$ so that we obtain

$$\frac{1}{s} = [\hat{a}(s)+1]\left[\frac{1}{Ls+\gamma_0} + \frac{1}{2\sqrt{\gamma_0}}\left(1 - \frac{\gamma_0}{Ls+\gamma_0}\right)\right]. \quad (37)$$

From Eq. (37), one realizes the existence of a temporal scale $\tau = L/\sqrt{\gamma_0}$ separating two different regimes.

For $t \ll \tau$, $\hat{a}(s)+1 = 2\sqrt{\gamma_0}/s$ so that $c_0(t) = 2\sqrt{\gamma_0}t$ and $c_k(t) = 2\sqrt{\gamma_0}/\gamma_k$. The correlation function is

$$C(r,t) = 2\sqrt{\gamma_0}\frac{t}{L} + 2\sqrt{\gamma_0}\int_{-\pi}^{\pi}\frac{dk}{2\pi}\frac{e^{ikr}}{2[1-(1-\gamma_0/2)\cos(k)]}. \quad (38)$$

The first term is negligible because $t \ll \tau$. Hence $C(r)$ does not depend on time and decays exponentially with r. This is a quasistationary state with coexisting domains of fixed size. Such a regime lasts for a time τ which diverges for $L \rightarrow \infty$, so that in the thermodynamic limit the system remains asymptotically in this disordered state.

For $t \gg \tau$ instead, all $\hat{c}_k(s)$ vanish except $\hat{c}_0(s) = L/s$. Hence $C(r) = 1$ and the system becomes completely ordered. This is the asymptotic regime for a system of finite size.

Let us summarize the results obtained in this section. We have solved the dynamics of the voter model on an annealed small-world topology: in this way we have found that finite systems remain in a disordered state for a time proportional to their size, and then converge to the totally ordered configuration; infinite systems instead reach a disordered final stationary state, with a correlation function that decays exponentially over a distance ξ_p. For small values of p the correlation length ξ_p diverges as $p^{-1/2}$.

IV. NUMERICAL RESULTS

In order to validate the analytical results presented above, we have performed numerical simulations of the voter model both on the annealed and on the quenched Watts-Strogatz topology.

Figure 1 reports, for the annealed case, the temporal behavior of the fraction n_A of active bonds, i.e., the fraction of nearest neighbor sites with opposite values of σ, for $p=0.1$ and several values of L. After an initial decrease, typical of one-dimensional systems, a plateau sets in. The analytical treatment predicts such a preasymptotic regime to last for an interval proportional to L. The inset of Fig. 1 confirms the analytical finding.
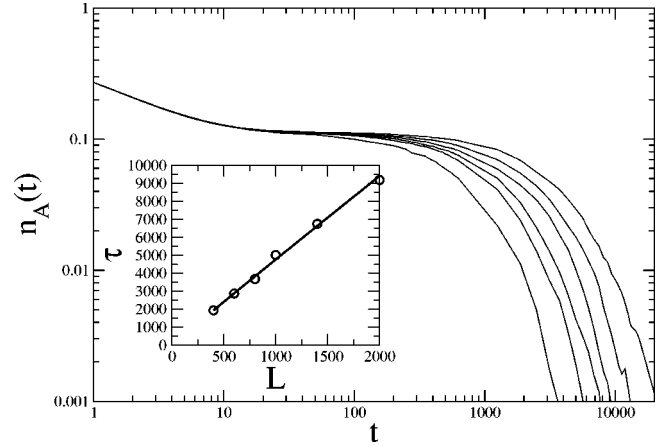

FIG. 1. Main: Plot of the fraction of active bonds n_A for $p=0.1$ and system sizes L 400, 600, 800, 1000, 1400, 2000 (from left to right) for the annealed case. Data are averaged over 1000 different realizations. Inset: The duration τ of the plateau in the main part of the figure (symbols) plotted vs L. τ is evaluated as the time at which n_A drops below 0.01. The straight line is a power-law regression with best-fit exponent equal to 0.98 ± 0.03.

In the limit $L \rightarrow \infty$, the disordered state corresponding to the plateau becomes the asymptotic one. The analytical solution predicts an exponential form of the correlation function [Eq. (26)] with the correlation length ξ_p given by Eq. (27). This analytical form is a very good approximation for the correlation function also for very large, but finite, values of L in the quasistationary regime ($t < \tau$). This is shown numerically in the main part of Fig. 2. In the inset of the same figure we report the values of ξ_p obtained numerically, which perfectly coincide with Eq. (27).

We have introduced the annealed version of the Watts-
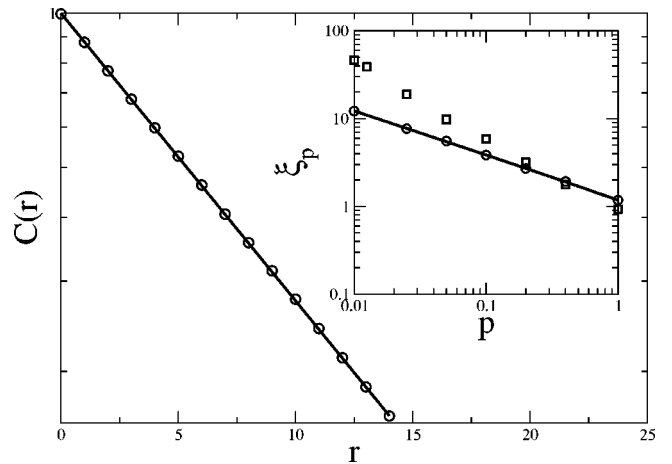

FIG. 2. Main: Correlation function $C(r)$ in the quasistationary state for a system of size $L=10^5$ and $p=0.025$ (symbols), compared with the analytical prediction, Eq. (26) (solid line). Only one realization of the noise is considered. The agreement is excellent. Inset: The correlation length ξ_p obtained numerically from the decay of the correlation function $C(r)$ in the quasistationary state of annealed WS networks with $L=10^5$ (circles), compared with the analytical prediction, Eq. (27) (solid line), and the same quantity computed for the quenched WS network (squares).
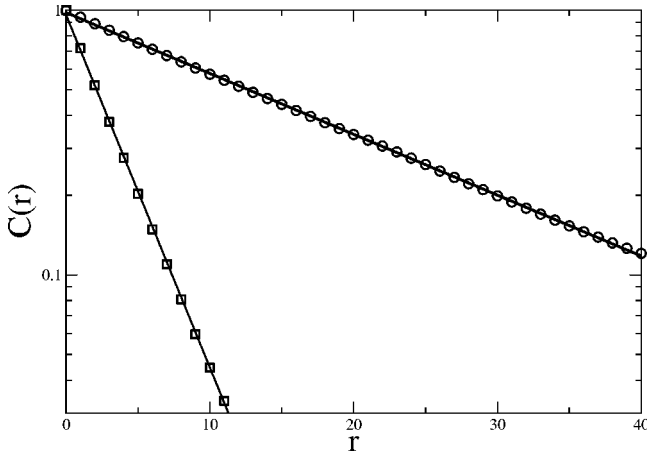
FIG. 3. Correlation function $C(r)$ in the quasistationary state for a quenched WS network of size $L=10^5$, $p=0.025$ (circles), and $p=0.2$ (squares). Only one realization is considered. The solid lines are exponential fits.

Strogatz network as an approximation for the WS network with quenched topology. Hence it is interesting to compare the results of the two cases to understand how well the approximation captures the behavior of the original system. In Ref. [9] we have already performed a numerical investigation of the voter dynamics on the quenched WS topology. By comparing the results reported in Ref. [9] and the theoretical approach presented here, we see that the annealed approximation correctly reproduces many of the important features of the original system, i.e., the existence of a regime with a disordered state before full order sets in and the linear dependence on L of the temporal scale τ between them. Concerning the shape of the final correlation function in the case of infinite quenched networks, Fig. 3 shows that $C(r)$ is exponential, another feature that is the same in the annealed and the quenched cases. What the annealed approximation is not able to capture is the quantitative dependence of the correlation length on p. This is shown in the inset of Fig. 2, where it is clear that, for small p, $\xi_p \sim p^{-1}$ in the quenched system [9], while $\xi_p \sim p^{-1/2}$ in the annealed case.

V. EXTENSION TO $\nu > 1$

In the previous sections we have considered an initial one-dimensional lattice with each site connected only to its nearest neighbors. When the number of neighbors connected to each site is $\nu > 1$, one can quite easily extend the analytical calculations presented above. On physical grounds one expects the qualitative picture to remain the same. Also formulas are very similar. In general they involve, in the place of f_2 and f_3, the functions $f_{2\nu}(p/L, L-1-2\nu)$ and $f_{2\nu+1}(p/L, L-2-2\nu)$. The equation for the average total magnetization becomes

$$\frac{dM}{dt} = [-1 + 2\nu f_{2\nu}(p/L, L-1-2\nu) + (L-1 \\ -2\nu)p/L f_{2\nu+1}(p/L, L-2-2\nu)]M, \quad (39)$$

and M is again conserved due to the vanishing of the coefficient on the right-hand side [Eq. (A4)]. The equation for the correlation function $C(r)$ becomes

$$\dot{C}(r) = -2\left(1 + \frac{pf_{2\nu+1}}{L}\right)C(r) + 2\left(f_{2\nu} - \frac{pf_{2\nu+1}}{L}\right)$$

$$\times \sum_{i=1}^{\nu} [C(r+i) + C(r-i)] + 2\frac{pf_{2\nu+1}}{L}\sum_{l=0}^{L-1}C(l). \quad (40)$$

Considering the continuum limit of Eq. (40) and looking for the stationary state one obtains

$$C'' - \lambda_L^2 C + \Phi_L = 0, \quad (41)$$

where now

$$\lambda_L^2 = \frac{(1-2\nu f_{2\nu})[1+(2\nu+1)/(L-2\nu-1)]}{[f_{2\nu} - (1-2\nu f_{2\nu})/(L-2\nu-1)]\omega_\nu} > 0 \quad (42)$$

and

$$\omega_\nu = \sum_{j=1}^{\nu} j^2 = \frac{\nu(\nu+1)(2\nu+1)}{6}. \quad (43)$$

Again the only solution for finite L is the completely ordered state $C(r) = 1$, while in the thermodynamic limit $C(r) = \exp[-\lambda(p)r]$. The correlation length is

$$\xi_p = 1/\lambda(p) = \frac{1}{\sqrt{1/F_{2\nu}(p) - 2\nu}}, \quad (44)$$

where $F_{2\nu}(p) = \lim_{L\to\infty}f_{2\nu}(p/L, L-2\nu-1)$. In the limit of small p, by expanding Eq. (A2), one finds

$$\xi_p \sim (2\nu p)^{-1/2}. \quad (45)$$

For what concerns the preasymptotic dynamics, the only formal change in Eq. (29) is that f_3 is replaced by $f_{2\nu+1}$, but now the form of γ_k is different,

$$\gamma_k = 2\left[1 + \frac{pf_{2\nu+1}}{L} - 2\left(f_{2\nu} - \frac{pf_{2\nu+1}}{L}\right)\sum_{j=1}^{\nu}\cos(jk)\right]. \quad (46)$$

By applying the Laplace transform one gets an equation formally equal to Eq. (36). For generic ν we cannot perform explicitly the integral appearing in Eq. (36) and hence we cannot write down the analog of Eq. (37). However, we can guess that the only change will be the replacement of the factor $1/2\sqrt{\gamma_0}$ with some other factor independent of L. Therefore the existence of two regimes separated by a temporal scale τ proportional to L will be preserved. Moreover, on physical grounds, we expect the proportionality factor to scale as $p^{-1/2}$ also for generic ν. To confirm this, we have performed numerical simulations of a system with next-nearest neighbor connections ($\nu = 2$). The results, presented in Fig. 4, confirm the expectation. The temporal scale τ sepa-
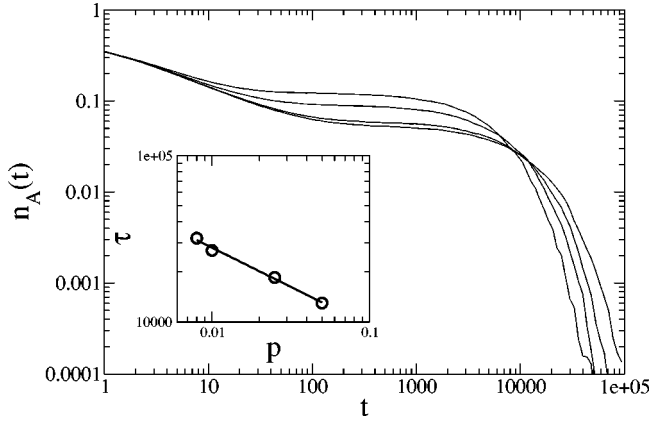
FIG. 4. Main: Plot of the fraction of active bonds n_A for $L = 3000$, and $p = 0.05$, $p = 0.025$, $p = 0.01$, and $p = 0.008$ (from top to bottom) for the annealed case. Data are averaged over 1000 different realizations. Inset: The duration τ of the plateau in the main part of the figure (symbols) plotted vs p. τ is evaluated as the time at which n_A drops below one-tenth of the value during the plateau. The straight line is a power-law regression with best-fit exponent equal to 0.47 ± 0.03.

rating the quasistationary disordered state from the totally ordered configuration scales as $Lp^{-1/2}$. We can conclude that the behavior of the voter model on the small-world topology is qualitatively the same, regardless of the number ν of connections between neighbors.

VI. CONCLUSIONS

In this paper we have studied analytically the voter model on the small-world topology. We have considered an annealed version of the Watts-Strogatz network, where long-range connections are not fixed, but chosen randomly at each time step. In this way each realization of the voter model dynamics takes place in an effective average small-world topology, and this allows the exact solution of the equation for the correlation function of the system.

The dynamical behavior of the model on the annealed topology is very similar to the behavior on the quenched WS network. Systems of finite size converge asymptotically to a totally ordered frozen state after an intermediate quasistationary stage, characterized by a finite correlation length. The duration of this preasymptotic regime is proportional to the number of sites. Hence systems of infinite size never reach the ordered state and remain in a disordered stationary state with finite domain size. All these features are exactly the same both on the annealed and on the quenched versions of the network. A quantitative difference arises only in the dependence of the correlation length ξ_p on the probability p of having a long-range connection. This discrepancy is not surprising, since a similar disagreement between the annealed and the quenched case has been noted previously for diffusion on Watts-Strogatz networks [20] and the voter model is well known to be related with first passage properties of random walkers [18]. In that case, the crossover time separating short and long time behavior of the mean number of distinct sites visited scales as p^{-2} in the quenched network

and as $1/p$ in the annealed one. This difference is due to the fact that in the quenched case a walker has to diffuse over a distance $1/p$ before reaching a shortcut and deviating from the one-dimensional behavior. This clearly requires a time p^{-2}. In the annealed case instead, the time needed to perform a long-range jump scales as $1/p$. In the voter model on small-world topology the boundaries between ordered domains perform a one-dimensional random walk for short times. The behavior changes when the walkers make a long-range jump. As mentioned above, this requires a time $1/p$ in the annealed network and p^{-2} in the quenched one. This difference generates the different scaling of the correlation length in the two types of topology.

Despite this discrepancy the voter model dynamics on small-world networks is relatively insensitive to the quenched or annealed nature of the topology. An interesting question for future work is whether this insensitivity extends also to other ordering processes on other complex networks.

APPENDIX

In this appendix we give explicit formulas for the functions $f_{2\nu}(p/L, L - 2\nu - 1)$ and $f_{2\nu+1}(p/L, L - 2\nu - 2)$. Let us consider

$$f_R(\alpha, N) \equiv \sum_{n=0}^{N} \binom{N}{n} \frac{\alpha^n (1-\alpha)^{N-n}}{R+n}. \tag{A1}$$

For $\alpha \neq 0$,

$$f_R(\alpha, N) = \frac{1}{\alpha^R} \int_0^\alpha ds \, s^{R-1} (s + 1 - \alpha)^N. \tag{A2}$$

The derivation of Eq. (A2) is easy:

$$
\begin{aligned}
f_R(\alpha, N) &= \frac{1}{\alpha^R} \sum_{n=0}^{N} \binom{N}{n} \frac{\alpha^{n+R}(1-\alpha)^{N-n}}{R+n} \frac{1}{\alpha^R} \\
&= \sum_{n=0}^{N} \binom{N}{n} (1-\alpha)^{N-n} \int_0^\alpha ds \, s^{R+n-1} \frac{1}{\alpha^R} \\
&= \int_0^\alpha ds \, s^{R-1} \sum_{n=0}^{N} \binom{N}{n} (1-\alpha)^{N-n} s^n \frac{1}{\alpha^R} \\
&= \int_0^\alpha ds \, s^{R-1} (s + 1 - \alpha)^N. \tag{A3}
\end{aligned}
$$

Using Eq. (A1) it is easy to verify that

$$R f_R(\alpha, N-R) + \alpha(N-R) f_{R+1}(\alpha, N-R-1) = 1. \tag{A4}$$

The vanishing of the coefficient on the right-hand side of Eqs. (18) and (39) is obtained by setting $R = 2\nu$, $\alpha = p/L$ and $N = L - 1$.

Using Eq. (A2) the explicit formulas for f_2 and f_3 are readily found to be

$$f_2(p/L, L-3) = \left(\frac{L}{p}\right)^2 \left[\frac{1}{L-1} - \frac{(1-p/L)}{L-2} + \frac{(1-p/L)^{L-1}}{(L-2)(L-1)}\right],$$
(A5)

$$f_3(p/L, L-4) = \left(\frac{L}{p}\right)^3 \left[\frac{1}{L-1} - \frac{2(1-p/L)}{L-2} + \frac{(1-p/L)^2}{L-3}\right.$$
$$\left. - \frac{2(1-p/L)^{L-1}}{(L-3)(L-2)(L-1)}\right].$$
(A6)

Finally the asymptotic forms of the functions for $L \to \infty$ are

$$F_2(p) = \lim_{L \to \infty} f_2(p/L, L-3) = \frac{1}{p} - \frac{(1-e^{-p})}{p^2}$$
(A7)

and

$$F_3(p) = \lim_{L \to \infty} f_3(p/L, L-4) = \frac{1}{p} - \frac{2}{p^2} + \frac{2(1-e^{-p})}{p^3},$$
(A8)

which go to 1/2 and 1/3, respectively, in the limit $p \to 0$.

---

[1] R. Albert and A.-L. Barabási, Rev. Mod. Phys. **74**, 47 (2002).

[2] M.E.J. Newman, SIAM Rev. **45**, 167 (2003).

[3] R. Axelrod, J. Conflict Resolut. **41**, 203 (1997).

[4] C. Castellano, M. Marsili, and A. Vespignani, Phys. Rev. Lett. **85**, 3536 (2000).

[5] K. Sznajd-Weron and J. Sznajd, Int. J. Mod. Phys. C **11**, 1157 (2000).

[6] P.L. Krapivsky and S. Redner, Phys. Rev. Lett. **90**, 238701 (2003).

[7] D. Boyer and O. Miramontes, Phys. Rev. E **67**, 035102 (2003).

[8] K. Klemm, V.M. Eguiluz, R. Toral, and M. San Miguel, Phys. Rev. E **67**, 026120 (2003).

[9] C. Castellano, D. Vilone, and A. Vespignani, Europhys. Lett. **63**, 153 (2003).

[10] D.J. Watts and S.H. Strogatz, Nature (London) **393**, 440 (1998).

[11] T. M. Liggett, *Interacting Particle Systems* (Springer, New York, 1985).

[12] P.L. Krapivsky, Phys. Rev. A **45**, 1067 (1992).

[13] L. Frachebourg, and P.L. Krapivsky, Phys. Rev. E **53**, 3009 (1996).

[14] R. Dickman and R. Vidigal, J. Phys. A **35**, 1147 (2002).

[15] F. Slanina and H. Lavicka, Eur. Phys. J. B **35**, 279 (2003).

[16] R. Monasson, Eur. Phys. J. B **12**, 555 (1999).

[17] R. Glauber, J. Math. Phys. **4**, 294 (1963).

[18] S. Redner, *A Guide to First-Passage Processes* (Cambridge University Press, Cambridge, 2001), pp. 136–139.

[19] A.J. Bray, J. Phys. A **22**, L67 (1989).

[20] J. Lahtinen, J. Kertész, and K. Kaski, Physica A **311**, 571 (2002).